Isoflurane inhibits synaptic vesicle exocytosis through reduced Ca^{2+} influx, not Ca^{2+}-exocytosis coupling

Joel P. Baumgart[a,1], Zhen-Yu Zhou[a,1], Masato Hara[a,b], Daniel C. Cook[a], Michael B. Hoppa[c,d], Timothy A. Ryan[a,c], and Hugh C. Hemmings Jr.[a,e,2]

[a]Department of Anesthesiology, Weill Cornell Medical College, New York, NY 10065; [b]Department of Anesthesiology, Kurume University School of Medicine, Kurume, Fukuoka 830-0011, Japan; [c]Department of Biochemistry, Weill Cornell Medical College, New York, NY 10065; [d]Department of Biology, Dartmouth College, Hanover, NH 03755; and [e]Department of Pharmacology, Weill Cornell Medical College, New York, NY 10065

Edited by Donald W. Pfaff, The Rockefeller University, New York, NY, and approved August 12, 2015 (received for review January 9, 2015)

Identifying presynaptic mechanisms of general anesthetics is critical to understanding their effects on synaptic transmission. We show that the volatile anesthetic isoflurane inhibits synaptic vesicle (SV) exocytosis at nerve terminals in dissociated rat hippocampal neurons through inhibition of presynaptic Ca^{2+} influx without significantly altering the Ca^{2+} sensitivity of SV exocytosis. A clinically relevant concentration of isoflurane (0.7 mM) inhibited changes in $[Ca^{2+}]_i$ driven by single action potentials (APs) by 25 ± 3%, which in turn led to 62 ± 3% inhibition of single AP-triggered exocytosis at 4 mM extracellular Ca^{2+} ($[Ca^{2+}]_e$). Lowering external Ca^{2+} to match the isoflurane-induced reduction in Ca^{2+} entry led to an equivalent reduction in exocytosis. These data thus indicate that anesthetic inhibition of neurotransmitter release from small SVs occurs primarily through reduced axon terminal Ca^{2+} entry without significant direct effects on Ca^{2+}-exocytosis coupling or on the SV fusion machinery. Isoflurane inhibition of exocytosis and Ca^{2+} influx was greater in glutamatergic compared with GABAergic nerve terminals, consistent with selective inhibition of excitatory synaptic transmission. Such alteration in the balance of excitatory to inhibitory transmission could mediate reduced neuronal interactions and network-selective effects observed in the anesthetized central nervous system.

GCaMP3 | pHlourin | mechanisms of anesthesia | live cell imaging | presynaptic

The molecular and cellular mechanisms of anesthetic-induced amnesia, unconsciousness and immobilization are incompletely understood, particularly for the modern halogenated ether derivatives like isoflurane. General anesthetics, which are essential to both medical practice and experimental neuroscience, have potent and selective effects on neurotransmission (1), including both presynaptic actions (reduced neurotransmitter release) and postsynaptic actions (modulation of receptor function). These effects contribute to anesthetic-induced reductions in neuronal interactions, which are critical to information processing and consciousness (2–4). Knowledge of the fundamental synaptic effects of anesthetics is therefore essential to a molecular and physiological understanding of anesthetic mechanisms, and to development of more selective and safer anesthetics.

Although postsynaptic electrophysiological effects of anesthetics can be assessed directly using whole cell recordings and heterologous expression of putative molecular targets, their presynaptic actions have been difficult to resolve by conventional approaches that do not clearly discriminate between presynaptic and postsynaptic contributions. Direct evidence for presynaptic effects of volatile anesthetics includes selective inhibition of glutamate release from isolated nerve terminals (5, 6) and of synaptic vesicle (SV) exocytosis in intact hippocampal neurons (7). However, it remains controversial whether these effects involve direct inhibition of SV exocytosis itself or of upstream targets (8, 9). Moreover, the mechanism for the greater sensitivity of glutamate release relative to that of other transmitters is unclear.

Neurotransmitter release is supralinearly dependent on presynaptic Ca^{2+} influx due to the highly cooperative binding of Ca^{2+} to synaptotagmin 1, the principal neuronal Ca^{2+} sensor for triggering vesicular fusion through increases in the probability of exocytosis (Pv) (10, 11). We used sensitive quantitative fluorescence imaging approaches to characterize the effects of the widely used volatile anesthetic isoflurane on the Ca^{2+} sensitivity of SV exocytosis in cultured rat hippocampal neurons. Although glutamate and GABA have distinct postsynaptic actions, differences in the mechanisms and regulation of SV exocytosis from glutamatergic and GABAergic neurons are not well characterized. Because previous studies indicate that glutamate release is more sensitive to inhibition by volatile anesthetics than GABA release (12), we compared the effects of isoflurane on the coupling of Ca^{2+} influx to exocytosis in glutamatergic and GABAergic boutons. Our results indicate that the inhibition of SV exocytosis by isoflurane is driven by a reduction in Ca^{2+} influx. This reduction occurs without affecting the apparent sensitivity of exocytosis to Ca^{2+}. Sensitivity of SV exocytosis to isoflurane is therefore determined by presynaptic targets upstream of exocytosis that determine the magnitude of action potential-evoked Ca^{2+} influx. Identification of neurotransmitter-selective effects of anesthetics on SV exocytosis is critical for understanding their pathway specific effects on neuronal interactions (13, 14).

Results

The effects of isoflurane on SV exocytosis were examined using the chimeric reporters of exocytosis vGlut-pHluorin (vG-pH) or synapto-pHlourin (syn-pH) expressed in dissociated rat hippocampal neurons in the presence of 2 or 4 mM extracellular Ca^{2+} ($[Ca^{2+}]_e$). In resting terminals the pHluorin moiety residing in the acidic SV lumen is quenched, but fluoresces upon exocytosis

Significance

Clarification of the presynaptic actions of general anesthetics is critical to understanding the molecular and cellular mechanisms of their prominent effects on synaptic transmission. We show that the ether anesthetic isoflurane inhibits synaptic vesicle exocytosis through inhibition of presynaptic Ca^{2+} influx in the absence of significant alteration of the Ca^{2+} sensitivity of exocytosis. The greater inhibition of glutamate release compared with GABA release is explained by the relative anesthetic resistance of Ca^{2+} influx in GABAergic boutons, consistent with overall reduction in excitatory synaptic tone.

Author contributions: J.P.B., Z.-Y.Z., M.B.H., and H.C.H. designed research; J.P.B., Z.-Y.Z., M.H., and D.C.C. performed research; T.A.R. contributed new reagents/analytic tools; J.P.B., Z.-Y.Z., M.H., D.C.C., and H.C.H. analyzed data; and J.P.B., Z.-Y.Z., T.A.R., and H.C.H. wrote the paper.

The authors declare no conflict of interest.

This article is a PNAS Direct Submission.

[1]J.P.B. and Z.-Y.Z. contributed equally to this work.

[2]To whom correspondence should be addressed. Email: hchemmi@med.cornell.edu.

NEUROSCIENCE

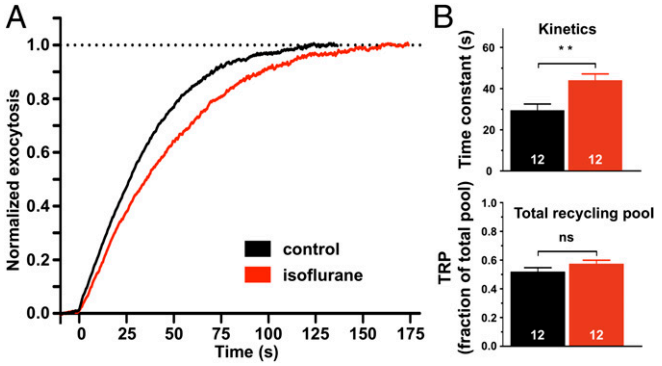

Fig. 1. Effects of isoflurane on synaptic vesicle recycling pool size and exocytosis kinetics. (*A*) Synaptic vesicle exocytosis kinetics were determined by fitting vGlut-pHluorin fluorescence traces during prolonged action potential (AP) stimulation in the presence of bafilomycin A1 (10 Hz for 150 s; 1,500 APs) for control or 0.7 ± 0.06 mM isoflurane [twice the minimum alveolar concentration (MAC); equivalent to EC_{50} for immobilization in rat] in the presence of 2 mM extracellular Ca^{2+} ($[Ca^{2+}]_e$). (*B*) (*Upper*) Effect of isoflurane on mean exocytosis time constant. Traces were fit with a single exponential function to determine the time constant for exocytosis of the recycling pool. $^{**}P < 0.01$ by two-tailed unpaired *t* test. (*Lower*) Effect of isoflurane on total recycling pool (TRP) size as a fraction of total pool size (determined using 50 mM NH_4Cl), $P = 0.21$ by two-tailed unpaired *t* test. $n = 12$.

with luminal alkalization. The reporter is then recycled via local endocytosis and the fluorescence signal is quenched upon reacidification by the V-type H^+ ATPase in the SV membrane (15). Action potential stimulation (1,500 APs at 10 Hz) in the presence of the H^+ ATPase inhibitor bafilomycin A1 provides a measure of the kinetics of exocytosis of the total recycling vesicle pool (TRP; Fig. 1*A*) (16).

Isoflurane [0.7 mM; twice the minimum alveolar concentration (MAC) equivalent to the EC_{50} for rat; ref. 17] significantly slowed exocytosis kinetics of the total recycling pool (TRP) (mean exocytosis time constants: $\tau_{control} = 29 \pm 3$ s, $n = 12$; $\tau_{isoflurane} = 44 \pm 3$ s, $n = 12$, 95% CI [4.6, 25]; Fig. 1*B*). Effective TRP size is a dynamic variable modulating synaptic performance (18); however the effects of isoflurane were limited to effects on exocytosis kinetics with no change in TRP size as a fraction of the total pool size (control 0.51 ± 0.03; isoflurane 0.57 ± 0.03; 95% CI [−0.14, 0.03]) determined by perfusion with 50 mM NH_4Cl to alkalize all vesicles (Fig. 1*B*).

We applied stimulation with AP trains of shorter duration to more closely mimic physiological conditions. A brief burst of AP firing (100 AP at 10 Hz) led to a rapid rise in vG-pH fluorescence (Fig. 2 *A* and *B*) corresponding to exocytosis of 0.25 ± 0.026 of the TRP. The average 100-AP response (ΔF_{100AP}) was inhibited by 55% to 0.11 ± 0.018 of TRP by 0.7 mM isoflurane (95% CI [−0.07, −0.21]; Fig. 2*B*). Single bouton analysis showed that essentially all boutons were inhibited, but the degree of inhibition was variable across the entire population of presynaptic boutons (Fig. 2*D*).

To narrow the possible mechanisms involved in inhibition of SV exocytosis, we examined the effect of isoflurane on exocytosis driven by single AP stimuli. Isoflurane markedly inhibited SV exocytosis in response to 1 AP from 0.015 ± 0.003 of TRP to 0.0049 ± 0.0009 of TRP (mean inhibition 62 ± 3%; 95% CI [−0.003, −0.016]) at 4 mM $[Ca^{2+}]_e$ (Fig. 3 *A* and *B*). Inhibition was completely reversible: Removal of isoflurane restored exocytosis to control levels (Fig. 3*A*). Given the cooperative nature of Ca^{2+} activation of neurotransmitter release, we investigated the effect of isoflurane on the Ca^{2+} dependence of SV exocytosis in response to a single AP stimulus at varied external Ca^{2+} concentrations. Single AP-evoked exocytosis was strongly enhanced by elevating $[Ca^{2+}]_e$, saturating at high $[Ca^{2+}]_e$ (Fig. 3*B*). Isoflurane significantly inhibited exocytosis at all Ca^{2+} concentrations. The effect of isoflurane on SV exocytosis elicited by a single AP stimulus (Fig. 3) was comparable to that elicited by multiple-AP trains (Fig. 2).

Strong inhibition of single AP-triggered exocytosis implies that isoflurane acts either on Ca^{2+} entry through voltage-gated Ca^{2+} channels or on SV fusion in response to increased presynaptic $[Ca^{2+}]_i$. We examined the impact of isoflurane on single-AP driven Ca^{2+} influx (18, 19) using the genetically-encoded Ca^{2+} indicator syn-GCaMP3 (20). Isoflurane reduced the linearized syn-GCaMP3 response by 30% from 1.2 ± 0.09 to 0.82 ± 0.06 at 4 mM $[Ca^{2+}]_e$ (95% CI [−0.13, −0.66]; Fig. 4 *A* and *B*), which indicates that isoflurane inhibits AP-triggered Ca^{2+} influx (18, 21). Using single AP-triggered activation with $[Ca^{2+}]_e$ from 1.5 to 10 mM, Ca^{2+} influx saturated at high $[Ca^{2+}]_e$, similar to previous findings in the hippocampus (21) and calyx of Held (22) (Fig. 4*B*). Isoflurane significantly inhibited Ca^{2+} influx over this entire range of $[Ca^{2+}]_e$, which is consistent with a noncompetitive mechanism of action with respect to $[Ca^{2+}]_e$. We next examined inhibition Ca^{2+} influx over a range of isoflurane concentrations (with $[Ca^{2+}]_e = 4$ mM). Isoflurane inhibited single AP-evoked Ca^{2+} influx in a concentration-dependent manner with $IC_{50} = 1.4 \pm 1.0$ mM (Fig. 4*C*). Significant inhibition occurred within the clinically relevant concentration range of 0.175 mM to 0.70 mM (defined as 0.5–2 × MAC).

These experiments strongly suggest that isoflurane inhibits SV exocytosis by reducing Ca^{2+} influx as reported by changes in single AP-triggered syn-GCaMP3 signals. We tested this hypothesis in two ways. First, we examined the cooperative relationship of single AP-triggered Ca^{2+} influx to SV exocytosis, which is well described by a generalized Hill equation: exocytosis = $[Ca^{2+}]_i^n/(K^n + [Ca^{2+}]_i^n)$ (18, 21) that effectively quantifies the efficiency of exocytosis at different degrees of Ca^{2+} influx (Fig. 5*A*). If isoflurane inhibits exocytosis purely by inhibiting AP-driven Ca^{2+} entry, then the same quantitative relationship should hold. The paired isoflurane data fell on the control curve, which indicates that the effect of isoflurane on SV exocytosis can be attributed to reductions in $[Ca^{2+}]_i$ without significant contributing effects

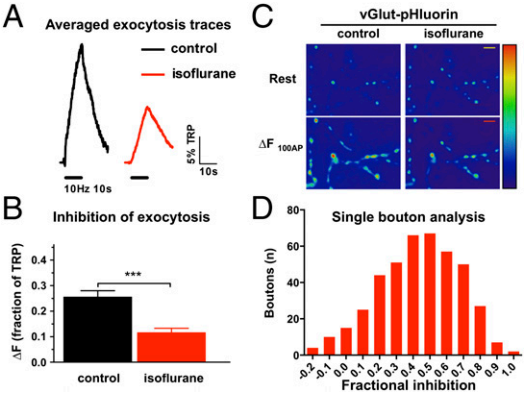

Fig. 2. Isoflurane inhibits synaptic vesicle exocytosis evoked by a brief action potential train. (*A*) Ensemble average traces of a vGlut–pHluorin transfected neuron stimulated at 10 Hz for 10 s (100 APs). Fluorescence intensities were normalized to the peak of a subsequent bafilomycin A1 response (defining the total recycling pool, TRP). (*B*) Mean values of vGlut–pHluorin response amplitudes for control or 0.7 ± 0.06 mM isoflurane-treated neurons stimulated with 100 APs in the presence of 2 mM extracellular Ca^{2+} ($[Ca^{2+}]_e$). Average 100 AP response (ΔF_{100AP}) was inhibited 55% by isoflurane, $^{***}P < 0.001$ by paired *t*-test, $n = 8$. (*C*) Representative field of vGlut–pHluorin fluorescence images at rest and difference image for 100 AP stimulation (ΔF_{100AP}) for control or isoflurane-treated neurons. (Scale bars: 5 μm.) (*D*) Histogram of fractional block of vGlut–pHluorin responses in single boutons stimulated with 100 AP. Measurements from 497 boutons collected in eight experiments.

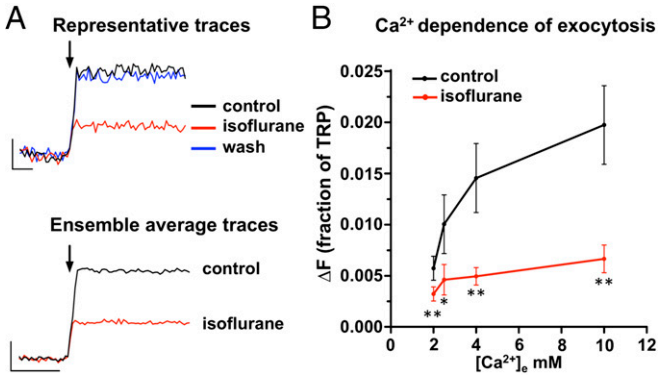

Fig. 3. Reversibility of isoflurane inhibition and Ca^{2+} dependence of synaptic vesicle exocytosis. (*A*) (*Upper*) Representative vGlut–pHlourin fluorescence responses elicited by a single AP at 4 mM extracellular Ca^{2+} ($[Ca^{2+}]_e$) for control (black), 0.7 mM isoflurane (red), and wash (blue) conditions. Arrow indicates single AP stimulus (n = 8 trials each, ~25 boutons analyzed per neuron). (*Lower*) Ensemble average traces of vGlut-pHlourin responses relative to total releasable pool (TRP) size to single AP stimulation at 4 mM extracellular Ca^{2+} ($[Ca^{2+}]_e$) (10 trial average, ~25 boutons per neuron). (Scale bar: 0.5% TRP, 100 ms.) (*B*) Isoflurane inhibition of single AP-stimulated release is not overcome by elevated extracellular Ca^{2+} ($[Ca^{2+}]_e$). Average relative peak (ΔF) evoked by a single AP stimulus expressed as a fraction of the TRP (n = 7–11). *P < 0.05, **P < 0.01 compared with respective control by paired t test. Mean isoflurane concentration 0.70 ± 0.06 mM.

on the Ca^{2+}-sensitivity of exocytosis. Second, if inhibition of Ca^{2+} influx is sufficient to explain reduced exocytosis, then simply lowering $[Ca^{2+}]_e$ should mimic the effect of isoflurane on the syn-GCaMP3 signal and replicate isoflurane inhibition of exocytosis. Reducing $[Ca^{2+}]_e$ from 4 mM to 2 mM reduced exocytosis from 0.0146 ± 0.0033 of TRP to 0.0057 ± 0.0012 of TRP (61 ± 8% inhibition; 95% CI [−0.0010, −0.0166]), which was comparable to inhibition by 0.7 mM isoflurane to 0.0049 ± 0.0009 of TRP at 4 mM $[Ca^{2+}]_e$ (62 ± 3% inhibition; 95% CI [−0.0034, −0.0158]; 95% CI for difference between 2 mM $[Ca^{2+}]_e$ and 4 mM $[Ca^{2+}]_e$ + isoflurane [−0.0023, 0.0039]; Fig. 5*B*, and see above Fig. 3). Similarly, lowering $[Ca^{2+}]_e$ from 4 mM to 2 mM reduced the syn-GCaMP3 signal from 1.1 ± 0.06 to 0.92 ± 0.02 linearized GCaMP3 units (by 16 ± 2%; 95% CI [−0.030, −0.314]), comparable to the reduction produced by 0.7 mM isoflurane to 0.82 ± 0.06 at $[Ca^{2+}]_e$ = 4 mM (by 25 ± 3%; 95% CI [−0.181, −0.363]; 95% CI for difference between 2 mM $[Ca^{2+}]_e$ and 4 mM $[Ca^{2+}]_e$ + isoflurane [−0.054, 0.254]; Fig. 5*C*).

To compare the effects of isoflurane on SV exocytosis from glutamatergic or GABAergic neurons separately, we used live-cell imaging of GABAergic boutons identified by vGAT–Oyster 550 immunolabeling (23) (Fig. 6*A*). Single AP-evoked SV exocytosis was measured by syn-pH and Ca^{2+} influx by syn-GCaMP3 (Fig. 6*B*) averaged over multiple trials (10–15) across populations of glutamatergic or GABAergic synapses. Individual glutamatergic boutons (vGAT-negative) exhibited greater inhibition by isoflurane than did GABAergic boutons (vGAT-positive) of peak syn-pH (62% compared with 38% inhibition; 95% CI [−13, −34]) and syn-GCaMP3 fluorescence (26% compared with 9% inhibition; 95% CI [−10, −24]) (Fig. 6*B*). For both neurotransmitter phenotypes, the effect of isoflurane on Ca^{2+} influx correlated with its effect on exocytosis over a range of $[Ca^{2+}]_e$, indicative of a minimal direct effect on the Ca^{2+} sensitivity of exocytosis (Fig. 6*C*). The Ca^{2+} sensitivity of SV exocytosis for glutamatergic or GABAergic boutons was not significantly different. Isoflurane shifted the frequency-response histogram for fractional inhibition of Ca^{2+} influx further to the right in glutamatergic boutons compared with GABAergic boutons (Fig. 6*D*).

Discussion

Using sensitive and specific assays of presynaptic anesthetic effects, we find that the widely used ether anesthetic isoflurane inhibits AP-evoked SV exocytosis without affecting the coupling between Ca^{2+} influx and exocytosis in mature cultured rat hippocampal neurons. Analysis of individual nerve terminals and neurons allowed us to isolate presynaptic mechanisms of isoflurane on exocytosis without interference from intrinsic neuronal networks or postsynaptic effects. A single AP stimulus provides a very brief local increase in intracellular free Ca^{2+}, allowing for high time resolution observations of presynaptic responses. Isoflurane inhibition of SV exocytosis measured using pHluorin indicators correlated with reduced Ca^{2+} influx measured using syn-GCaMP3; there were no direct effects on the Ca^{2+} sensitivity of SV exocytosis. By varying $[Ca^{2+}]_e$, we observed that the Ca^{2+} dependence of SV exocytosis follows the same supralinear relationship in the presence or absence of isoflurane. Moreover, isoflurane inhibited SV exocytosis from glutamatergic boutons more potently than from GABAergic boutons in proportion to the reduction in presynaptic Ca^{2+} influx. This presynaptic selectivity was not due to an intrinsic difference in the Ca^{2+} sensitivity of exocytosis between glutamatergic and GABAergic terminals, which were in fact similar in control conditions. These findings elucidate fundamental synaptic mechanisms that lead to neurotransmitter-selective effects that are critical to understanding the actions of anesthetics on sensitive neuronal networks (13, 14).

Neurotransmitter release is determined by the highly cooperative relationship between Ca^{2+} entry and SV exocytosis, and by the number of docked and primed vesicles (readily releasable pool) (24). Ca^{2+} entry is regulated mainly by presynaptic ion channels (e.g., Na^+, Ca^{2+}, and K^+ channels), presynaptic receptors, and modulatory cell signaling mechanisms (25). We have shown previously that isoflurane has transmitter-specific

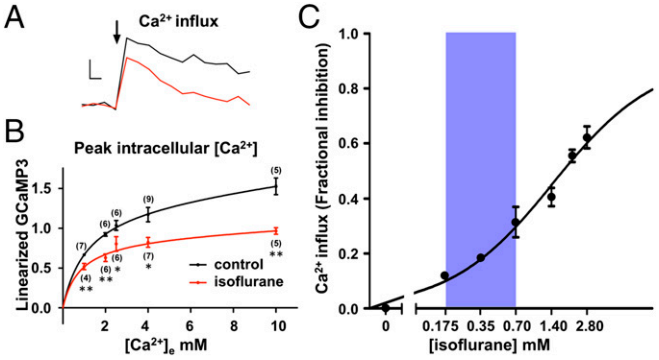

Fig. 4. Isoflurane reduces action potential-stimulated increases in presynaptic Ca^{2+} influx. (*A*) Control (black) and 0.70 ± 0.06 mM isoflurane (red) ensemble average traces of single AP-evoked $[Ca^{2+}]$ influx determined by linearized responses synaptophysin–GCaMP3 at 4 mM extracellular Ca^{2+} ($[Ca^{2+}]_e$). Arrow indicates single AP stimulus. (Scale bar: 30% $\Delta F/F_0$, 100 ms.) (*B*) Inhibition by 0.70 ± 0.06 mM isoflurane of average peak $\Delta F/F_0$ evoked by single AP stimulus as a function of $[Ca^{2+}]_e$. Data are fitted to a single site binding model using a Levenberg–Marquardt algorithm optimization method (control: EC_{50} = 1.3 ± 0.1 mM, E_{max} = 1.6 ± 0.5, R^2 = 99.8; isoflurane: EC_{50}= 0.8 ± 0.4 mM, E_{max} = 0.9 ± 0.2, R^2 = 92.3); both P < 0.05 by two-sample sum-of-squares F test comparison against the null hypothesis that E_{max} and EC_{50} values are identical. (*C*) Inhibition of Ca^{2+} influx as a function of log [isoflurane] using synaptopysin-GCaMP3 at 4 mM $[Ca^{2+}]_e$ (n = 27). Shaded area indicates the clinical concentration range of isoflurane for general anesthesia in rat (0.18–0.7 mM; 0.5–2 × MAC). Data are fitted to a generalized Hill model by least-squares analysis (I_{max} = 0.92 ± 0.17; IC_{50} = 1.4 ± 1.0 mM). Inhibition data were all significantly different from paired control values (*P < 0.05 in two-tailed paired t test).

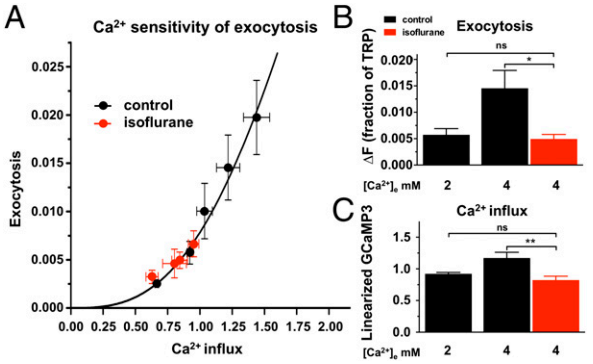

Fig. 5. Effect of isoflurane on synaptic vesicle exocytosis as a function of Ca^{2+} influx. (*A*) Exocytosis determined using synaptophysin-pHlourin ($\Delta F/F$) in response to a single AP stimulus relative to total releasable pool (TRP) at 1.5, 2, 2.5, 4, 10 mM $[Ca^{2+}]_e$ is plotted against Ca^{2+} influx determined using synaptophysin-GCaMP3 (ΔF) under similar conditions in the absence or presence of 0.70 ± 0.06 mM isoflurane to reveal the Ca^{2+} sensitivity of exocytosis (n = 34 for syn-pH experiments, n = 28–33 for syn-GCaMP3 experiments). Data are fitted to a generalized Hill model [exocytosis = $[Ca^{2+}]_i^n/(K^n+[Ca^{2+}]_i^n)$, n = 2.9 ± 0.5, K = 2.8 ± 0.2]. (*B*) Reduction of $[Ca^{2+}]_e$ from 4 mM to 2 mM mimicked the reduction in exocytosis produced by 0.70 ± 0.06 mM isoflurane at 4 mM $[Ca^{2+}]_e$. *P < 0.05 by one-way ANOVA with Tukey's post hoc test. (*C*) Reduction of $[Ca^{2+}]_e$ from 4 mM to 2 mM mimicked the reduction in syn-GCaMP3 signal produced by 0.70 ± 0.06 mM isoflurane at 4 mM $[Ca^{2+}]_e$. **P < 0.01 by one-way ANOVA with Tukey's post hoc test.

effects on neurotransmitter release from a heterogeneous population of isolated axon terminals (26), and inhibits chemically evoked glutamate release more potently than release of other neurotransmitters (12, 26). Pharmacological differences between glutamate and GABA release could result from synapse-specific differences in expression and/or coupling of specific isoforms of ion channels or other proteins regulating SV exocytosis (27, 28). Hippocampal glutamate and GABA containing SVs differ in their release properties during AP trains as well as in their adaptive response to strong depolarization (29–31). Different profiles of presynaptic ion channel expression underlie exocytosis in glutamatergic and GABAergic synapses (32–34). Our findings that greater isoflurane sensitivity of glutamatergic compared with GABAergic SV exocytosis is determined by larger effects on Ca^{2+} influx are consistent with transmitter phenotype-specific differences in expression of the presynaptic ion channels that determine $[Ca^{2+}]_i$, including distinct subtypes of Na_v, Ca_v, and K_v channels (35).

Greater sensitivity of glutamate release to anesthetic inhibition is consistent with a net reduction in network excitability involving both presynaptic and postsynaptic inhibition of glutamatergic transmission. The relative anesthetic insensitivity of GABA release coupled with the potent anesthetic potentiation of postsynaptic $GABA_A$ receptors (1) and increased asynchronous GABA release (36) together enhance net hippocampal network inhibition (37). The balance of anesthetic actions on overall network excitability can vary between brain regions, consistent with synaptic and regional differences in anesthetic target expression and/or functional roles (38). The presynaptic selectivity of volatile anesthetics like isoflurane in suppressing excitatory neurotransmission is expected to scale up to reduced neuronal interactions and information transfer at the network level, which is considered a leading mechanism for anesthetic-induced unconsciousness (2, 39).

The molecular mechanisms of general anesthetics involve effects on both excitatory and inhibitory synaptic transmission (1). Potentiation of $GABA_A$ receptors represents the major action of most i.v. anesthetics (40, 41), but this mechanism alone does not account for the lesser target selectivity of volatile anesthetics compared with i.v. anesthetics (42, 43). Potential synaptic volatile anesthetic targets involved in regulating transmitter release include glutamate receptors, Na_v channels (44), K_{2P} channels (45), nicotinic acetylcholine receptors (34), Ca_v channels (46), neurotransmitter transporters (47, 48), and SNARE proteins (8, 49). Evidence suggests that the presynaptic effects of volatile anesthetics on neurotransmitter release are mediated by reduced nerve terminal excitability from inhibition of Na_v channels rather than direct inhibition of Ca^{2+} influx by inhibition of Ca_v channels (7, 44, 50, 51). A critical distinction is between presynaptic reductions in Ca^{2+} influx involving direct inhibition of Ca_v (e.g., 52) or indirect effects involving alterations in the presynaptic AP waveform as a result of effects on other ion channels including K_v and Na_v (35, 50, 51, 53). We have previously shown that hippocampal neuron SV exocytosis is much less sensitive to isoflurane when evoked by elevated extracellular KCl to open Ca_v rather than by electrical simulation of action potentials (7), which provides further support for a major target upstream of Ca^{2+} entry. Recent enhancements in the use of microbial rhodopsin-based indicators of membrane voltage that are sensitive and fast enough to detect presynaptic APs (54, 55) will facilitate tests of this hypothesis by allowing quantification of anesthetic effects on AP properties in individual hippocampal boutons.

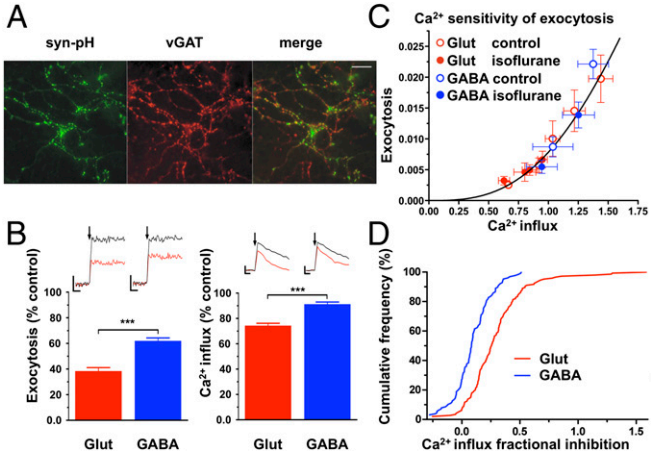

Fig. 6. Differential effects of isoflurane on synaptic vesicle exocytosis in glutamatergic and GABAergic neurons is proportional to reduction Ca^{2+} influx. (*A*) Representative live-cell image of syn-pH-positive boutons (green, *Left*), GABAergic boutons immunolabeled using vGAT–Oyster 550 (red, *Center*), and merge shown as yellow (*Right*), with surrounding vGAT-positive boutons (red, *Right*) from untransfected neurons. (Scale bar: 20 μm.) (*B Left*) The effect of 0.70 ± 0.06 mM isoflurane on single AP exocytosis is greater in glutamatergic (vGAT-negative; 62 ± 3% block, n = 11) than in GABAergic (vGAT-positive; 38 ± 3% block, n = 5) boutons at 4 mM extracellular $[Ca^{2+}]_e$, ***P < 0.001 by unpaired t test. (*Insets*) Exemplar single AP stimulus (arrow) syn-pH fluorescence traces before (black) and after (red) isoflurane in glutamatergic (*Left*) and GABAergic (*Right*) boutons. (Scale bars: 0.5% TRP, 100 ms.) (*B, Right*) Effect of isoflurane on presynaptic Ca^{2+} influx is greater in glutamatergic (26 ± 2% block, n = 7) than in GABAergic (9.2 ± 2% block, n = 7) boutons at 4 mM extracellular $[Ca^{2+}]_e$, ***P < 0.001 by unpaired t test. (*Insets*) Exemplar single AP stimulus (arrow) syn-GCaMP3 fluorescence traces before (black) and after (red) isoflurane in glutamatergic and GABAergic boutons. (Scale bars: 30% $\Delta F/F_0$, 200 ms.) (*C*) Effect of 0.70 ± 0.06 mM isoflurane on exocytosis as a function of Ca^{2+} influx in glutamatergic and GABAergic boutons. Exocytosis determined using syn-pH in response to single AP relative to TRP is plotted against relative increases in Ca^{2+} influx determined using syn-GCaMP3 over a range of $[Ca^{2+}]_e$ from 1.5 to 10 mM under similar conditions to yield the Ca^{2+} sensitivity of exocytosis (n = 26 for exocytosis, n = 24 for Ca^{2+} influx). The curve indicates the data from Fig. 5*A*. (*D*) Cumulative frequency distribution of 0.70 ± 0.06 mM isoflurane inhibition of peak $[Ca^{2+}]_i$ for GABAergic and glutamatergic boutons. Data from 272 boutons collected in 12 experiments.

The observation that isoflurane inhibits SV exocytosis in a way that is quantitatively consistent with reductions in Ca^{2+} influx indicates anesthetic target(s) upstream of Ca^{2+}-exocytosis coupling. Our findings in intact hippocampal neurons using sensitive and direct assays of SV fusion and Ca^{2+} influx support isoflurane effects on AP-evoked increases in $[Ca^{2+}]_i$ as the principal presynaptic mechanism of action. In contrast, studies using reduced cell preparations (permeabilized pheochromocytoma cells) have suggested direct effects of isoflurane on SNARE-mediated SV fusion (8, 9). This discrepancy might be in part due to the use of permeabilized tumor cells to measure release of catecholamines, which is known to involve different mechanisms compared with typical small SVs, including distinct Ca^{2+} sensitivity of SV vesicle exocytosis (56). Whether these differences represent transmitter-specific differences in release from large dense core vesicles in pheochromocytoma cells compared with release from small SVs in hippocampal neurons (26, 55) or artifacts due to use of detergents and ionophores for membrane permeabilization (8, 9) will require confirmation in intact catecholamine-releasing neurons using live cell imaging approaches. Our findings appear to contradict a report that isoflurane inhibits ionomycin-evoked RH414 destaining of rat hippocampal neuron boutons with no change in neuronal $[Ca^{2+}]$ (9). However, the measurements of whole cell peak $[Ca^{2+}]$ reported using fura 2 reflect primarily changes in somatic rather than nerve terminal $[Ca^{2+}]$, and involve contributions from distinct Ca^{2+} sources and combinations of Ca^{2+} channel subtypes due to differences in subcellular expression (57).

Several factors must be considered in interpreting these results. Experiments were performed at 30 °C to facilitate recording stability and pharmacological analysis. The kinetics of SV exocytosis and endocytosis are faster at higher physiological temperatures, but exhibit similar fundamental properties (58). Cultured hippocampal neurons provide an accessible model for analyzing nerve terminal physiology, but they lack the tissue structure of slice preparations and therefore might not fully reflect properties of typical hippocampal neuron terminals in situ. Differences in isoflurane effects on SV exocytosis from other neuronal types and in other brain regions must also be considered (26).

Our findings indicate that isoflurane reduces presynaptic Ca^{2+} influx preferentially in glutamatergic compared with GABAergic boutons imply that at least one of the key molecular players controlling AP-driven Ca^{2+} influx is different in these two neuronal subtypes. Further studies are required to identify these molecular target(s) for isoflurane inhibition (26), but the studies presented here significantly narrow the list of possibilities. Volatile anesthetics have multiple cellular actions including depression of glutamate-mediated excitatory transmission and facilitation of inhibitory GABAergic transmission, in contrast to the principally GABAergic i.v. anesthetics propofol and etomidate that selectively potentiate $GABA_A$ receptors (1, 13, 59). Although both propofol and the volatile anesthetic sevoflurane produce similar frontal coherent alpha and slow electroencephalographic oscillations in vivo, probably due to shared GABAergic mechanisms mediating amnesia and unconsciousness, sevoflurane has additional distinct encephalographic effects consistent with non-GABAergic actions (60). The depressive effects of isoflurane on hippocampal CA1 neuron excitability in rat brain slices involve primarily nonGABAergic mechanisms including direct depression of glutamate-mediated excitation (61), which supports an important role for effects on glutamatergic transmission. A nonGABAergic mechanism such as suppression of excitatory transmission through Na_v channel blockade (42, 43, 62) is likely to mediate isoflurane-induced immobility, a ventral spinal anesthetic endpoint (63). At higher doses, inhibition of glutamatergic transmission likely contributes to electroencephalographic silence in vivo (64, 65). Clarification of such fundamental molecular and cellular mechanisms for the synaptic selectivity of volatile anesthetics such as isoflurane in depressing excitatory neurotransmission presynaptically while enhancing inhibitory neurotransmission postsynaptically provides a framework for explaining the higher order neuronal network processes relevant to specific anesthetic endpoints including amnesia, unconsciousness and immobility (13, 14).

Materials and Methods

Materials and Solutions. Cells were perfused at 0.27 mL min^{-1} with Tyrode's solution (119 mM NaCl, 2.5 mM KCl, 1.5–10 mM $CaCl_2$, 25 mM Hepes buffered to pH 7.4, 30 mM glucose) containing 10 μM 6-cyano-7-nitroquinoxaline-2,3-dione (CNQX) and 50 μM D,L-2-amino-5-phosphonovaleric acid (AP5). Isoflurane dissolved in Tyrode's solution was perfused focally onto imaged cells via a 150-μm-diameter pipette; delivered isoflurane concentrations were determined by gas chromatography (66).

Neuron Imaging. Experiments were approved by the Weill Cornell Medical College Institutional Animal Care and Use Committee and conformed to NIH Guidelines for the Care and Use of Animals. Hippocampal CA3–CA1 regions were dissected from neonatal Sprague–Dawley rats, and cells were dissociated, plated, and transfected as described (67). Live-cell imaging was performed at 30.0 ± 0.2 °C using an epifluorescence microscope (ZEISS Axio Observer Z1). Synaptophysin-pHluorin (syn-pH), was used as an optical sensor of SV exocytosis (68, 69); for experiments requiring higher signal-to-noise ratio, vGlut-pHluorin (vG-pH) was used (58). Synaptophysin-GCaMP3 (syn-GCaMP3) was used to measure intracellular Ca^{2+} ($[Ca^{2+}]_i$) in hippocampal neuron boutons stimulated by field-potential-generated APs. Fluorescence images were acquired with an Andor iXon1 camera (model DU-897E-BV) with a solid-state diode pumped 488-nm laser.

Exocytosis and Calcium Measurements. For exocytosis, ΔF of syn-pH and vG-pH was determined as the difference between the average of 10 frames before and after a single AP stimulus. Signals were expressed as a fraction or percentage of TRP, determined by applying a maximally depleting stimulus (1,500 APs at 10 Hz) in the presence of bafilomycin A1 (Fig. 1). Superfusion of 0.7 mM isoflurane for 5 min did not affect baseline fluorescence or maximal fluorescence elicited by 1,500 APs in the presence of bafilomycin A (TRP; $\Delta F <$ 4%) of either syn-pH or vG-pH transfected boutons. For Ca^{2+} influx, ΔF of syn-GCaMP3 was determined as the difference between the average of 10 frames before and the 5 highest points after a single AP stimulus. Changes in fluorescence were normalized to syn-GCaMP intensity at Ca^{2+} saturation (F_{MAX}) determined by applying 200 μM ionomycin, which caused a 6.1- to 6.6-fold increase in syn-GCaMP3 fluorescence in agreement with previous results (19). Changes in GCaMP3 fluorescence ($\Delta F/F$) are related to changes in intracellular Ca^{2+} according to a generalized Hill equation ($V_{max} = 1$, $k =$ 9.077, $n = 2.5$; adjusted $R^2 = 0.997$; ref. 19), and can be linearized to the single AP signal obtained using the linear indicator Magnesium Green (Life Technologies) as $(\Delta F/F)_{linear} = (((\Delta F/F)/F_{MAX}) \times k^n)/(1 - ((\Delta F/F)/F_{MAX}))^{(1/n)}$. Superfusion of 0.7 mM isoflurane for 5 min did not affect baseline fluorescence ($\Delta F < 4\%$) of syn-GCaMP3 transfected boutons.

Image and Data Analysis. Images were analyzed in ImageJ (rsb.info.nih.gov/ij) using a custom plugin (rsb.info.nih.gov/ij/plugins/time-series.html). Rabbit vGAT-Oyster 550 luminal domain antibody was used to identify GABAergic neurons (23). Values are shown as mean ± SEM. ANOVA with Tukey's post hoc test, Student's or Welch's unpaired *t* test ($P < 0.05$), and 95% confidence intervals on the difference of the means were used to determine statistical significance.

ACKNOWLEDGMENTS. We thank L. Looger, Y. Zhu, S. Voglmaier, and R. Edwards for generously providing plasmids, and members of the H.C.H. and T.A.R. laboratories for constructive comments. This work was supported by National Institutes of Health Grants T32DA07274 (to J.P.B.), R01MH085783 (to T.A.R.), and R01GM58055 (to H.C.H.).

1. Hemmings HC, Jr, et al. (2005) Emerging molecular mechanisms of general anesthetic action. *Trends Pharmacol Sci* 26(10):503–510.
2. Alkire MT, Hudetz AG, Tononi G (2008) Consciousness and anesthesia. *Science* 322(5903):876–880.
3. Lewis LD, et al. (2012) Rapid fragmentation of neuronal networks at the onset of propofol-induced unconsciousness. *Proc Natl Acad Sci USA* 109(49):E3377–E3386.
4. Blain-Moraes S, et al. (2015) Neurophysiological correlates of sevoflurane-induced unconsciousness. *Anesthesiology* 122(2):307–316.

5. Schlame M, Hemmings HC, Jr (1995) Inhibition by volatile anesthetics of endogenous glutamate release from synaptosomes by a presynaptic mechanism. *Anesthesiology* 82(6):1406–1416.
6. Miao N, Frazer MJ, Lynch C, 3rd (1995) Volatile anesthetics depress Ca^{2+} transients and glutamate release in isolated cerebral synaptosomes. *Anesthesiology* 83(3): 593–603.
7. Hemmings HC, Jr, Yan W, Westphalen RI, Ryan TA (2005) The general anesthetic isoflurane depresses synaptic vesicle exocytosis. *Mol Pharmacol* 67(5):1591–1599.
8. Herring BE, Xie Z, Marks J, Fox AP (2009) Isoflurane inhibits the neurotransmitter release machinery. *J Neurophysiol* 102(2):1265–1273.
9. Xie Z, et al. (2013) Interaction of anesthetics with neurotransmitter release machinery proteins. *J Neurophysiol* 109(3):758–767.
10. Augustine GJ (2001) How does calcium trigger neurotransmitter release? *Curr Opin Neurobiol* 11(3):320–326.
11. Chapman ER (2008) How does synaptotagmin trigger neurotransmitter release? *Annu Rev Biochem* 77:615–641.
12. Westphalen RI, Hemmings HC, Jr (2006) Volatile anesthetic effects on glutamate versus GABA release from isolated rat cortical nerve terminals: 4-aminopyridine-evoked release. *J Pharmacol Exp Ther* 316(1):216–223.
13. Franks NP (2008) General anaesthesia: From molecular targets to neuronal pathways of sleep and arousal. *Nat Rev Neurosci* 9(5):370–386.
14. Brown EN, Purdon PL, Van Dort CJ (2011) General anesthesia and altered states of arousal: A systems neuroscience analysis. *Annu Rev Neurosci* 34:601–628.
15. Sankaranarayanan S, De Angelis D, Rothman JE, Ryan TA (2000) The use of pHluorins for optical measurements of presynaptic activity. *Biophys J* 79(4):2199–2208.
16. Sankaranarayanan S, Ryan TA (2001) Calcium accelerates endocytosis of vSNAREs at hippocampal synapses. *Nat Neurosci* 4(2):129–136.
17. Taheri S, et al. (1991) What solvent best represents the site of action of inhaled anesthetics in humans, rats, and dogs? *Anesth Analg* 72(5):627–634.
18. Kim SH, Ryan TA (2010) CDK5 serves as a major control point in neurotransmitter release. *Neuron* 67(5):797–809.
19. Hoppa MB, Lana B, Margas W, Dolphin AC, Ryan TA (2012) $\alpha 2\delta$ expression sets presynaptic calcium channel abundance and release probability. *Nature* 486(7401): 122–125.
20. Tian L, et al. (2009) Imaging neural activity in worms, flies and mice with improved GCaMP calcium indicators. *Nat Methods* 6(12):875–881.
21. Ariel P, Ryan TA (2010) Optical mapping of release properties in synapses. *Front Neural Circuits* 4:1–10.
22. Schneggenburger R, Meyer AC, Neher E (1999) Released fraction and total size of a pool of immediately available transmitter quanta at a calyx synapse. *Neuron* 23(2): 399–409.
23. Dobie FA, Craig AM (2011) Inhibitory synapse dynamics: Coordinated presynaptic and postsynaptic mobility and the major contribution of recycled vesicles to new synapse formation. *J Neurosci* 31(29):10481–10493.
24. Dittman J, Ryan TA (2009) Molecular circuitry of endocytosis at nerve terminals. *Annu Rev Cell Dev Biol* 25:133–160.
25. Meir A, et al. (1999) Ion channels in presynaptic nerve terminals and control of transmitter release. *Physiol Rev* 79(3):1019–1088.
26. Westphalen RI, Desai KM, Hemmings HC, Jr (2013) Presynaptic inhibition of the release of multiple major central nervous system neurotransmitter types by the inhaled anaesthetic isoflurane. *Br J Anaesth* 110(4):592–599.
27. Bragina L, et al. (2011) Analysis of synaptotagmin, SV2, and rab3 expression in cortical glutamatergic and GABAergic axon terminals. *Front Cell Neurosci* 5:32.
28. Reid CA, Bekkers JM, Clements JD (2003) Presynaptic Ca^{2+} channels: A functional patchwork. *Trends Neurosci* 26(12):683–687.
29. Grønborg M, et al. (2010) Quantitative comparison of glutamatergic and GABAergic synaptic vesicles unveils selectivity for few proteins including MAL2, a novel synaptic vesicle protein. *J Neurosci* 30(1):2–12.
30. Moulder KL, et al. (2007) Vesicle pool heterogeneity at hippocampal glutamate and GABA synapses. *J Neurosci* 27(37):9846–9854.
31. Xu J, Mashimo T, Südhof TC (2007) Synaptotagmin-1, -2, and -9: Ca(2+) sensors for fast release that specify distinct presynaptic properties in subsets of neurons. *Neuron* 54(4):567–581.
32. Rahamimoff R, et al. (1999) Multitude of ion channels in the regulation of transmitter release. *Philos Trans R Soc Lond B Biol Sci* 354(1381):281–288.
33. Vacher H, Mohapatra DP, Trimmer JS (2008) Localization and targeting of voltage-dependent ion channels in mammalian central neurons. *Physiol Rev* 88(4):1407–1447.
34. Martire M, et al. (2010) Pre-synaptic BK channels selectively control glutamate versus GABA release from cortical and hippocampal nerve terminals. *J Neurochem* 115(2): 411–422.
35. Debanne D, Bialowas A, Rama S (2013) What are the mechanisms for analogue and digital signalling in the brain? *Nat Rev Neurosci* 14(1):63–69.
36. Pittson S, Himmel AM, MacIver MB (2004) Multiple synaptic and membrane sites of anesthetic action in the CA1 region of rat hippocampal slices. *BMC Neurosci* 5:52.
37. Bieda MC, MacIver MB (2004) Major role for tonic $GABA_A$ conductances in anesthetic suppression of intrinsic neuronal excitability. *J Neurophysiol* 92(3):1658–1667.
38. Oose Y, et al. (2012) Imbalanced suppression of excitatory and inhibitory synaptic transmission onto mouse striatal projection neurons during induction of anesthesia with sevoflurane in vitro. *Eur J Neurosci* 35(9):1396–1405.
39. Mashour GA (2014) Top-down mechanisms of anesthetic-induced unconsciousness. *Front Syst Neurosci* 8:115.
40. Sonner JM, et al. (2003) Inhaled anesthetics and immobility: Mechanisms, mysteries, and minimum alveolar anesthetic concentration. *Anesth Analg* 97(3):718–740.
41. Jurd R, et al. (2003) General anesthetic actions in vivo strongly attenuated by a point mutation in the GABA(A) receptor beta3 subunit. *FASEB J* 17(2):250–252.
42. Zhang Y, et al. (2004) Gamma-aminobutyric acidA receptors do not mediate the immobility produced by isoflurane. *Anesth Analg* 99(1):85–90.
43. Liao M, et al. (2005) Beta3-containing gamma-aminobutyric acidA receptors are not major targets for the amnesic and immobilizing actions of isoflurane. *Anesth Analg* 101(2):412–418.
44. Herold KF, Hemmings HC, Jr (2012) Sodium channels as targets for volatile anesthetics. *Front Pharmacol* 3:50.
45. Franks NP, Honoré E (2004) The TREK K2P channels and their role in general anaesthesia and neuroprotection. *Trends Pharmacol Sci* 25(11):601–608.
46. Study RE (1994) Isoflurane inhibits multiple voltage-gated calcium currents in hippocampal pyramidal neurons. *Anesthesiology* 81(1):104–116.
47. Westphalen RI, Hemmings HC, Jr (2003) Effects of isoflurane and propofol on glutamate and GABA transporters in isolated cortical nerve terminals. *Anesthesiology* 98(2):364–372.
48. Cechova S, Zuo Z (2006) Inhibition of glutamate transporters increases the minimum alveolar concentration for isoflurane in rats. *Br J Anaesth* 97(2):192–195.
49. Nagele P, et al. (2005) Volatile anesthetics bind rat synaptic snare proteins. *Anesthesiology* 103(4):768–778.
50. Wu XS, Sun JY, Evers AS, Crowder M, Wu LG (2004) Isoflurane inhibits transmitter release and the presynaptic action potential. *Anesthesiology* 100(3):663–670.
51. Ouyang W, Hemmings HC, Jr (2005) Depression by isoflurane of the action potential and underlying voltage-gated ion currents in isolated rat neurohypophysial nerve terminals. *J Pharmacol Exp Ther* 312(2):801–808.
52. Joksovic PM, et al. (2009) Isoflurane-sensitive presynaptic R-type calcium channels contribute to inhibitory synaptic transmission in the rat thalamus. *J Neurosci* 29(5): 1434–1445.
53. Rama S, Zbili M, Debanne D (2014) Modulation of spike-evoked synaptic transmission: The role of presynaptic calcium and potassium channels. *Biochim Biophys Acta* 1853(9):1933–1939.
54. Hochbaum DR, et al. (2014) All-optical electrophysiology in mammalian neurons using engineered microbial rhodopsins. *Nat Methods* 11(8):825–833.
55. Hoppa MB, Gouzer G, Armbruster M, Ryan TA (2014) Control and plasticity of the presynaptic action potential waveform at small CNS nerve terminals. *Neuron* 84(4): 778–789.
56. Verhage M, et al. (1991) Differential release of amino acids, neuropeptides, and catecholamines from isolated nerve terminals. *Neuron* 6(4):517–524.
57. Elliott EM, Malouf AT, Catterall WA (1995) Role of calcium channel subtypes in calcium transients in hippocampal CA3 neurons. *J Neurosci* 15(10):6433–6444.
58. Balaji J, Ryan TA (2007) Single-vesicle imaging reveals that synaptic vesicle exocytosis and endocytosis are coupled by a single stochastic mode. *Proc Natl Acad Sci USA* 104(51):20576–20581.
59. Solt K, Forman SA (2007) Correlating the clinical actions and molecular mechanisms of general anesthetics. *Curr Opin Anaesthesiol* 20(4):300–306.
60. Akeju O, et al. (2014) Effects of sevoflurane and propofol on frontal electroencephalogram power and coherence. *Anesthesiology* 121(5):990–998.
61. MacIver MB (2014) Anesthetic agent-specific effects on synaptic inhibition. *Anesth Analg* 119(3):558–569.
62. Zhang Y, et al. (2010) Bidirectional modulation of isoflurane potency by intrathecal tetrodotoxin and veratridine in rats. *Br J Pharmacol* 159(4):872–878.
63. Jinks SL, Bravo M, Hayes SG (2008) Volatile anesthetic effects on midbrain-elicited locomotion suggest that the locomotor network in the ventral spinal cord is the primary site for immobility. *Anesthesiology* 108(6):1016–1024.
64. Lukatch HS, Kiddoo CE, Maciver MB (2005) Anesthetic-induced burst suppression EEG activity requires glutamate-mediated excitatory synaptic transmission. *Cereb Cortex* 15(9):1322–1331.
65. Kenny JD, Westover MB, Ching S, Brown EN, Solt K (2014) Propofol and sevoflurane induce distinct burst suppression patterns in rats. *Front Syst Neurosci* 8:237.
66. Ratnakumari L, Hemmings HC, Jr (1998) Inhibition of presynaptic sodium channels by halothane. *Anesthesiology* 88(4):1043–1054.
67. Ryan TA (1999) Inhibitors of myosin light chain kinase block synaptic vesicle pool mobilization during action potential firing. *J Neurosci* 19(4):1317–1323.
68. Miesenböck G, De Angelis DA, Rothman JE (1998) Visualizing secretion and synaptic transmission with pH-sensitive green fluorescent proteins. *Nature* 394(6689):192–195.
69. Kim SH, Ryan TA (2009) A distributed set of interactions controls mu2 functionality in the role of AP-2 as a sorting adaptor in synaptic vesicle endocytosis. *J Biol Chem* 284(47):32803–32812.